Commensurate vortex lattices pinned by a periodic lattice of columnar defects



2000 J. Phys.: Condens. Matter 12 467

(http://iopscience.iop.org/0953-8984/12/4/307)

J. Phys.: Condens. Matter **12** (2000) 467–481. Printed in the UK PII: S0953-8984(00)03360-9

# Commensurate vortex lattices pinned by a periodic lattice of columnar defects

Yong-li Ma

Department of Physics, Fudan University, Shanghai 200433, People's Republic of China
and
Condensed Matter Group, International Centre for Theoretical Physics, 34100 Trieste, Italy

Received 13 April 1999, in final form 25 August 1999

**Abstract.** The effects of a periodic hexagonal lattice of columnar defects on the curves of magnetic induction $B(H)$, vortex-lattice melting $T_m(H)$ and critical current density $J_c(H)$ versus external field $H$ are investigated, including the effects of vortex interaction, thermal and quantum fluctuations, an applied current drive and columnar pin disorder. It is found theoretically that the smallest slope of $B(H)$ occurs when the magnetic induction $B$ matches the regular pinning field $n_{pin}\phi_0$ over a finite range of $H$. This commensuration leads to an inhibition of the vortex-lattice melting and a large enhancement of the critical current density, i.e., the curves of $T_m(H)$ and $J_c(H)$ each have a series of broad plateaus. The applied current drive, electric field-like in form, shifts this melting curve downwards. $J_c(T)$ is the power-3/2 temperature decay at intermediate temperatures and decays exponentially to zero at high temperatures. The pin disorder and ion straggling reduce these favourable effects and wash out the plateaus when they become equal to certain critical values.

## 1. Introduction

Columnar pinning sites produced by heavy-ion bombardment are known to pin vortex lines in a vortex liquid in high-temperature superconductors [1,2]. The ions produce quasi-cylindrical voids and other defects $\sim$7 nm in diameter; vortices of core size $\xi \sim 1$ nm can be bound to these columnar holes. The properties of random columnar pins and single-vortex lines forming a Bose glass have been studied theoretically [3]. For fields such that $B \simeq n_{pin}\phi_0$ where $n_{pin}$ is the pin density and $\phi_0$ the flux quantum, a maximum vortex-line pinning and a superconducting phase are postulated [3] (a Mott-insulating phase in terms of the vortex lines). On the other hand, below a vortex-lattice freezing–melting line [4–6], the liquid of vortices forms a lattice with compressional, tilt and shear elastic moduli [7] that play an important role in determining the melting line $T_m(H)$ estimated according to the Lindemann criterion. Of course, quantum fluctuations turn out to be quantitatively important except in the immediate vicinity of $T_c$ [8]. In general the weak point pinning is regarded as unimportant qualitatively, merely shifting the melting line downwards [9]. However, extended defects, such as twin boundaries of separation $\sim$140 $\mu$m, can produce large peaks of $J_c$ just below $T_m(H)$ [10]. An excellent review and rich supply of references including all of these features are given by Blatter *et al* [11]. Recently, some progress in vortex physics has been achieved [12]. The dynamics and pinning of the vortex lattice in a periodic potential have also attracted much attention [11,13–15]. For example, $J_c(H)$ peaks at matching magnetic fields have been observed for low-$T_c$ materials [16–18].

0953-8984/00/040467+15$30.00  

In this paper, I focus on the commensurability of vortex lattices with a regular lattice of columnar defects and investigate the effects of the columnar pins on the curves of magnetic induction $B(H)$, vortex-lattice melting $T_m(H)$ and critical current density $J_c(H)$, including the effects of vortex interaction, thermal and quantum fluctuations, columnar disorder and an applied current drive. The pins are modelled [13] by a periodic hexagonal lattice of harmonic well depths, and I am interested in the commensurate case of vortex lattices in registry with the periodic pinning potential. This corresponds to a Mott-insulator-like regime [3], but now in a vortex-lattice part of the phase diagram.

The model of periodic columnar pins is theoretically interesting in itself; a possible experimental method of producing such well-defined pinning arrays is also crucial. The question in experiments is that of how to choose the pinning parameter values of the periodicity $a_p$ (hole separation) and size $r_p$ (hole radius). The small values of the coherence length ($\xi \sim 1$ nm) and the large values of the Ginzburg–Landau parameter ($\kappa \equiv \lambda/\xi \sim 10^2$) for high-$T_c$ superconductors are essentially different from the corresponding values for conventional superconductors. High-$T_c$ superconductors are extreme type-II superconductors; the areal vortex density changes over many orders of magnitude on changing the magnetic field from one that is weaker than a lower critical field $H_{c1} \leqslant 10^{-2}$ T up to the upper critical field $H_{c2} \sim 10^2$ T. What is the best working value of $B$? From $B \sim H$, the values of $10^{-1}$–$10^1$ in T for high-$T_c$ superconductors and $10^0$–$10^1$ in G for conventional superconductors, the commensurability of vortex lattices with a periodic columnar pin lattice is of major importance. To ensure that $B \sim B_\Phi$ ($\equiv 2\phi_0/\sqrt{3}a_p^2$), we require $a_p$ on the nanometre scale for high-$T_c$ superconductors and on the submicron scale for conventional superconductors. Experimentally, the regular lattices of holes in the conventional superconductors were prepared using lithographic techniques [19]. A regular nanometre-scale pin lattice has been made in an 'island' type of artificial-pinning-centre superconducting composite wire [20] and such lattices have unusually good superconducting properties. For example, the pins are extremely regular in positioning and shape for $r_p = 46$ nm and the critical size for the regular pins is $r_p \simeq 15$ nm. Furthermore, when $r_p$ went from a large size down to 7.5 nm, the matching field $B_\Phi \simeq 0.3$ T (corresponding to $a_p \simeq 81.6$ nm) was obtained. It is possible that a highly uniform, periodic lattice of vortex-pinning holes can be achieved near to the optimum vortex-pinning size for useful high-field superconductors. This periodic lattice of columnar pins in high-$T_c$ superconductors could be produced by ion beam irradiation through a mask that is drilled by a computer-controlled laser beam. Recently, introducing ordered arrays of columnar defects by means of electron irradiation [21], the enhancement of $J_c$ and matching effects in the pinning force density have been observed. Of course, the model presented in this paper is suitable for any values of microscopic pinning parameters, such as size $r_p$, periodicity $a_p$ and depth $V_p$, as long as they can be carefully controlled experimentally. Typical values of $r_p$, $a_p$ and $V_p$ are chosen for illustrating interesting issues.

The behaviour of the vortices is determined by the competition of the vortex interaction energy, pinning energy and thermal energy. Remarkably, the vortex interaction energy and pinning energy have the same order of magnitude below intermediate values of $T$ and have $1 - T/T_c$ and $(1 - T/T_c)^2$ dependencies at high $T$, respectively, as well as both vanishing at $T_c$. Thus in the physical picture this problem is described by two characteristic temperatures: the thermal excitation temperature $T_u$ required to eject the vortices out of the traps which, as a function of $T$ and $H$, is determined by the strength of the pinning energy and vortex interaction; and the melting temperature $T_{m0}$ in the absence of the pins which, as a function of $H$, is determined by the vortex interaction strength. For the strong-coupling case $T_u \gg T_{m0}$, at low temperatures $T \ll T_{m0}$ or low field $H \sim H_{c1}$, the vortices first form a commensurate state with all vortices trapped to look like a solid if the number of pins is larger than the number of

vortices. Otherwise, if the number of pins is less than the number of vortices, then a subset of the vortices are pinned and other vortices get out of the traps and still form a sublattice. For the intermediate-coupling case $T_u \sim T_m$, at $T \simeq T_{m0}$ or $H_{c1} \ll H \ll H_{c2}$, the vortices first form two subsets of the possible lattice and then melt the sublattice out of the traps at $T = T_{m0}$. For the weak-coupling case $T_u \ll T_m$, at $T \simeq T_m$ or $H \gg H_{c1}$, the vortices first get out of the traps and still form a lattice and then melt at $T = T_m$. Therefore the $B(H)$ curve, starting from the minimum of the Gibbs free-energy density $G$ with respect to $B$, shows a series of small-slope segments. The $T_m(H)$ and $J_c(H)$ curves, used for obtaining an extended Lindemann criterion and determined by the balance between the pinning force tending to keep the pinned vortex in the hole and the Lorentz force tending to detach every vortex from the ideal position, respectively, each show a series of plateaus over a broad range of $H$.

The main results are that:

(i) there are a series of small-slope (the slope even vanishes) $B(H)$ curves within the commensurate regions;
(ii) commensurate pinning inhibits vortex-lattice melting; the $T_m(H)$ line has a series of plateaus over a finite range of external field $H$;
(iii) an applied current encourages vortex-lattice melting $T_m(H, J) < T_m(H, 0)$ $(\equiv T_m(H))$;
(iv) $J_c(H)$ also has strongly enhanced plateaus due to the matching effects; $J_c(T)$ shows the usual power-3/2 decay at intermediate temperatures and exponential vanishing at high temperatures;
(v) positional disorder $\bar{\sigma}_p$ in the periodic pinning less than a critical disorder, $\bar{\sigma}_p < \bar{\sigma}_{pc}$, reduces these favourable effects and washes out the plateaus when $\bar{\sigma}_p = \bar{\sigma}_{pc}$.

This paper is organized as follows. Section 2 first describes the constitutive $B$–$H$ relation as the competition of hexagonal lattices between a vortex lattice and columnar pins. Section 3 develops the model as an elastic energy functional including the thermal and quantum fluctuations and periodic columnar pins with disorder. Section 4 evaluates the vortex-lattice melting curve $T_m(H)$, and presents the effects of a current drive on the melting curve $T_m(H, J)$ with and without pinning. Section 5 gives limiting estimates of the critical current density $J_c(H, T)$ with and without disorder. Section 6 gives a summary and conclusions.

## 2. The small-slope transition of vortex lattices

We shall assume that a regular lattice of vortex lines represents the most favourable configuration of type-II superconductors in the equilibrium state even though pin sites enable us to adjust the vortex lattice and induce multiple-flux quanta [22]. If one considers just the interactions between vortices, then a lattice of vortices parallel to the $z$-axis at the points $\{\boldsymbol{R}_i\}$ gives a two-dimensional magnetic field distribution which is proportional to $K_0(R_i/\lambda)$, a zero-order Hankel function of imaginary argument. The Gibbs free energy per unit volume without pinning takes the form [23]

$$G_A = \frac{H_{c1} - H}{8\pi} B + \frac{\phi_0 B}{32\pi^2\lambda^2} {\sum_i}' K_0\left(\frac{R_i}{\lambda}\right) \tag{1}$$

where the sum is over all vortices, excluding the one at the origin. The equilibrium value of $B$ is found by setting $\partial G_A/\partial B = 0$. An implicit equation for the constitutive relation $B = B(H)$ was obtained in inverse form [24]:

$$H = H_{c1} + \frac{\phi_0}{8\pi\lambda^2}\left[2\Sigma_0(\rho) + \frac{1}{2}\rho^2\Sigma_1(\rho)\right] \tag{2}$$

where

$$\Sigma_0(\rho) \equiv {\sum_{lm}}' K_0(\rho\mu_{lm}) \qquad \Sigma_1(\rho) \equiv 4\rho^2(\partial/\partial\rho^2)^2\Sigma_0(\rho) - {\sum_{lm}}' \mu_{lm}^2 K_0(\rho\mu_{lm})$$

$$\rho \equiv a_0/\lambda \qquad \mu_{lm} \equiv \sqrt{l^2 + lm + m^2}$$

with $l$ and $m$ integers for the periodic hexagonal vortex lattice. The distance $a_0$ between adjacent vortex lines is set by the average magnetic induction $B$. In practice, only square and hexagonal lattices have been considered, in which $B = \phi_0/a_0^2$ (square) and $B = 2\phi_0/\sqrt{3}a_0^2$ (hexagonal). Substituting equation (2) into equation (1), one has

$$G_A[B(H)] = -\frac{\phi_0 B\rho^2}{128\pi^2\lambda^2}\Sigma_1(\rho). \tag{3}$$

Like the results [24] for the square lattice, the above sums for the hexagonal lattice for the range $H_{c1} \leqslant H \leqslant H_{c2}$ may be easily obtained analytically. The results are

$$\Sigma_0(\rho) = \frac{4\pi}{\sqrt{3}\rho^2} + \frac{1}{2}\ln\left(\frac{\sqrt{3}\rho^2}{8\pi}\right) - A - \frac{3\sqrt{3}}{64\pi^3}{\sum_{lm}}' \frac{\rho^2}{\mu_{lm}^2(\mu_{lm}^2 + 3\rho^2/16\pi^2)}$$

with $A \simeq 0.17155$ and

$$\Sigma_1(\rho) = \frac{16\pi}{\sqrt{3}\rho^4} - \frac{2}{\rho^2} + \frac{3\sqrt{3}}{16\pi^3}{\sum_{lm}}' \frac{1}{(\mu_{lm}^2 + 3\rho^2/16\pi^2)^2}.$$

The analytical expressions for equations (2) and (3), defined as $H_A$ and $G_A$ for convenience, are given by

$$H_A = H_{c1} + B + \frac{\phi_0}{8\pi\lambda^2}\left[\ln\left(\frac{\phi_0}{4\pi\lambda^2 B}\right) - 2A - 1\right] - \frac{12\sqrt{3}\phi_0^3}{(4\pi\lambda)^6 B^2}{\sum_{l,m}}' \frac{1}{\mu_{lm}^2(\mu_{lm}^2 + \sqrt{3}\phi_0/8\pi^2\lambda^2 B)^2} \tag{4}$$

$$G_A[B(H_A)] = \frac{B}{16\pi^2}\left(\frac{\phi_0}{4\lambda^2} - B\right) - \frac{3\phi_0^2}{1024\pi^5\lambda^4}{\sum_{l,m}}' \frac{1}{(\mu_{lm}^2 + \sqrt{3}\phi_0/8\pi^2\lambda^2 B)^2}. \tag{5}$$

Equation (4) is just the Abrikosov curve in its inverse form $B(H)$ for all values of the external field such that $H_{c1} < H < H_{c2}$ in mean-field theory. The series in equation (4) converges rapidly, so five nearest neighbours are sufficient for obtaining an accuracy of five significant figures. This Abrikosov vortex lattice exists below the line of melting transitions $T_m(H)$. In this regime, thermal wandering of vortices can be neglected, and the vortices will be essentially straight, which allows us to ignore the elastic energy, especially in the pinning regions when the number of vortices is less than the number of pins.

On introducing a hexagonal lattice of columnar pins, one needs to consider the competition between this lattice and the hexagonal lattice of vortex lines. The $B$–$H$ Abrikosov curve is modified by the pinning energy term that lowers the energy close to commensurabilities. Using the rigid-rod approximation to focus on the main small-slope effects [13,25], the pinning energy is expressed in terms of a parabolic well of radius $r_p$ and depth $-\frac{1}{2}V_p$:

$$E_P = \begin{cases} \displaystyle\sum_{\text{occupied pins}} \frac{1}{2}V_p\left[\frac{|\boldsymbol{\delta}_{pi}|^2}{r_p^2} - 1\right] & \text{for } |\boldsymbol{\delta}_{pi}| < r_p \\ 0 & \text{for } |\boldsymbol{\delta}_{pi}| > r_p \end{cases} \tag{6}$$

where the pinning strength is determined by the solution of the Ginzburg–Landau equation for the vortex line [4] and has an interpolation formula $V_p = \varepsilon_0 \ln(1 + r_p^2/2\xi^2)$ with the elastic

energy per unit length [11] $\varepsilon_0 \equiv (\phi_0/4\pi\lambda)^2$. The vortex line with equilibrium position $\boldsymbol{R}_i$ is trapped by a single columnar pin centred at $\boldsymbol{R}_{pi}$ and $\boldsymbol{\delta}_{pi} = \boldsymbol{R}_i - \boldsymbol{R}_{pi}$.

The hexagonal vortex-lattice vectors $\{\boldsymbol{R}_i\}$ are of minimum scale $a_0$ and the competing hexagonal pinning-lattice vectors $\{\boldsymbol{R}_{pi}\}$ are of minimum scale $a_p$ with a 'matching field' $B_\Phi$ for this columnar pin lattice. The measure of columnar density commonly used is $B_\Phi = 2\phi_0/\sqrt{3}a_p^2$ with area density $n_{pin} \simeq a_p^{-2}$. In exact commensurate cases, $\{\boldsymbol{R}_{pi}\}$ is a subset of $\{\boldsymbol{R}_i\}$ if $a_0 = a_p/\mu_{lm}$ in the $B \geqslant B_\Phi$ regime, and $\{\boldsymbol{R}_i\}$ is a subset of $\{\boldsymbol{R}_{pi}\}$ if $a_p = a_0/\mu_{lm}$ in the $B < B_\Phi$ regime. We may take the equilibrium displacements $\delta_p \equiv a_p - a_0\mu_{lm}$ ($\delta_p \equiv a_p - a_0/\mu_{lm}$) to represent the average values of $|\delta_{pi}|$ in the $B \geqslant B_\Phi$ ($B < B_\Phi$) regime. The pinning potential is effective only for a finite range of fields $\Delta B_{lm} = B_{lm}^{(+)} - B_{lm}^{(-)}$ around the commensurate values $B_{lm} \equiv B_\Phi \mu_{lm}^{\pm 2}$, i.e., $|a_p - a_0\mu_{lm}^{\pm 1}| < r_p$, the vortex line inside a columnar hole, where the boundary values for $B$ are $B_{lm}^{(\pm)} = B_{lm}(1 \mp r_p/a_p)^{-2}$. The relative width around $B_{lm}$ is

$$\frac{\Delta B_{lm}}{B_{lm}} = \frac{4r_p}{a_p}\left[1 - \left(\frac{r_p}{a_p}\right)^2\right]^{-2} \ll 1. \tag{7}$$

The width increases with $B_{lm}$. For $\delta_p$ beyond $r_p$, the pinning contribution is zero, while for $\delta_p$ less than $r_p$, $E_P$ is quadratic in $\delta_p$. We introduce a factor $\nu$ which is defined as a ratio of the sum over occupied pins to the sum over all vortex-lattice sites. Thus for $B \geqslant B_\Phi$ ($B < B_\Phi$), every pin site is occupied (every vortex is pinned) and the factor $\nu$ is $\nu = a_0^2/a_p^2$ ($\nu = 1$). Only the occupied pin holes contribute to $E_P$, so the sum is over the pinned vortex sites. This leads to

$$\sum_{\text{occupied pins}} \cdots = \nu \sum_i \cdots$$

where the sum for $i = (l, m)$ is over all vortex lines in the $xy$-plane.

The total Gibbs free energy per unit volume becomes $G = G_A + G_P$, on adding the pinning energy contribution

$$G_P \equiv \frac{E_P}{\text{total areas}} \simeq \frac{\nu V_p B}{2\phi_0}\left(\frac{\delta_p^2}{r_p^2} - 1\right)\Theta(r_p - \delta_p)$$

with $\Theta(x)$ the Heaviside step function. Taking the minimum of $G$ with respect to $B$ at constant $T$ leads to the general relation $H = H_A + H_P$, with $H_A$ given by equation (4) and

$$H_P = \frac{4\pi}{\phi_0} V_p \Theta(r_p - \delta_p) \begin{cases} \left(\dfrac{a_p}{r_p}\right)^2 \dfrac{B_\Phi}{B}\sqrt{\dfrac{B_{lm}}{B}}\left(1 - \sqrt{\dfrac{B_{lm}}{B}}\right) & \text{for } B \geqslant B_\Phi \\ \left(\dfrac{a_p}{r_p}\right)^2 \left(1 - \sqrt{\dfrac{B_{lm}}{B}}\right) - 1 & \text{for } B < B_\Phi. \end{cases} \tag{8}$$

This modification is only for the range where vortices are at the pinning sites. From equation (8), one obtains $H_P \geqslant 0$ for $B \geqslant B_{lm}$ and $H_P < 0$ for $B < B_{lm}$ within the widths $\Delta B_{lm}$. Therefore, the slope of $B(H)$ within $\Delta B_{lm}$ becomes small. In particular, in the $B \simeq B_\Phi$ regime,

$$H_P = \begin{cases} 0 & \text{for } B = B_\Phi + 0 \\ -\dfrac{4\pi}{\phi_0} V_p & \text{for } B = B_\Phi - 0 \end{cases} \tag{9}$$

and the slope vanishes for an exact commensurate condition $B = B_\Phi$. This just represents 'Meissner'-like or 'Mott-insulator'-like transitions. In the two limit cases of $B \ll B_\Phi$ and $B \gg B_\Phi$, we get hardly any change and get back to the Abrikosov $B$–$H$ curve at best. Except for the small-slope transitions, are there any fixed-$B$ constant values $B = B_{lm}$ on the flat parts

of the $B$–$H$ curve? An answer to this question is suggested [13] by finding the minimum in the Gibbs free-energy branches. In fact, one only needs to discuss two possible competing branches of the general $G$ and special $G_c$ with

$$G_c \equiv G\big|_{B=B_{lm}} = G_A\big|_{B=B_{lm}} - \frac{\nu V_p B_{lm}}{2\phi_0}$$

within $|\Delta B_{lm}|$. If $\Delta G = G_c - G < 0$, then $B = B_{lm}$ lock-in occurs. To examine this, one extends the early $\Delta G$ calculation [13] to the exact-vortex-interaction case, and from equations (4), (5) and (8), it is easy to get

$$\begin{aligned}\Delta G = {} & \frac{B_{lm}^2}{16\pi}\left(\frac{B}{B_{lm}} - 1\right)^2 + \frac{\phi_0 B_{lm}}{(8\pi\lambda)^2}\left(1 - \frac{B}{B_{lm}} + \ln\frac{B}{B_{lm}}\right) + \frac{9\phi_0^2 a_p^2 B_\Phi}{(4\pi)^7\lambda^6 B_{lm}} \\ & \times {\sum_{l,m}}' \frac{(1 - B_{lm}/B)^2}{[\mu_{lm}^2 + 3B_\Phi a_p^2/(4\pi\lambda)^2 B_{lm}][\mu_{lm}^2 + 2\sqrt{3}\phi_0/(4\pi\lambda)^2 B]^2} + \frac{V_p}{\sqrt{3}r_p^2} \\ & \times \begin{cases} (B_{lm}/B_\Phi)^2[(B/B_{lm})^{1/4} - (B_{lm}/B)^{1/4}] & \text{for } B \geqslant B_\Phi \\ [1 - (B_{lm}/B)^{1/2}][2(B_{lm}/B)^{1/2} - (B_{lm}/B)^{3/2} - 1] & \text{for } B < B_\Phi. \end{cases}\end{aligned} \tag{10}$$

Every term on the right-hand side of equation (10) is greater than or equal to zero, except the second term in round brackets ($\leqslant 0$), resulting in $\Delta G \geqslant 0$ for all possible values of $B$. This shows conclusively that a periodic hexagonal lattice of columnar pins can give rise to a series of small-slope segments in the $B(H)$ curve within the matching regions, but the fixed-$B$ value $B = B_{lm}$ is only at $B = B_\Phi$ over a small range of $H$.

According to the minimum of the Gibbs free energy, the usual Abrikosov curve of $B(H)$ is followed with equation (4) until $H$ becomes equal to $H_{lm}^{(-)}$, when the vortex lattice enters the pinning region. The $B(H)$ curve then jumps to $B_{lm}^{(-)}$; the width $\Delta H = H_{lm}^{(+)} - H_{lm}^{(-)}$ is traversed by equations (4) and (8) with small slope within the widths $\Delta B_{lm}$ until $H$ reaches $H_{lm}^{(+)}$. The $B(H)$ curve then jumps back to the Abrikosov curve as the vortex lattice moves out of the pinning region. At low temperatures and high magnetic fields, the dependencies of $\lambda$ and $\xi$ on the temperature and field become [11, 26] $\zeta^2(t) = \zeta^2(0)/(1 - t - b)$ with $\zeta = (\lambda, \xi)$, the reduced temperature $t = T/T_c$, the reduced magnetic induction $b = B/H_{c2}(0)$ and the zero-temperature upper critical field $H_{c2}(0)$. For the choice of parameters $\lambda(0) = 100$ nm, $\xi(0) = 1.4$ nm, $H_{c2}(0) = 170$ T and $T_c = 92$ K for YBaCuO high-$T_c$ superconductors and taking the pin values $r_p = 7.5$ nm and $a_p = 50$ nm (corresponding to $B_\Phi = 8.28$ kG), figure 1 shows the $B$–$H$ curve at $T = 77$ K with three small-slope segments in $B_{lm} = (1/3, 1, 3)B_\Phi$ regions. These regions are those of the sublattices of hexagonal structures with commensurations $B_l = 3^l B_\Phi$ ($l = 0, \pm 1, \pm 2, \ldots$). For convenience, we use this $l$ from $B_l$ rather than $(l, m)$ from $B_{lm}$ to label the commensurate regions in figure 1. The 'Meissner'-like effect for $B = B_\Phi$ is very weak since $H \ll H_{c2}$ for high-$T_c$ superconductors. Although this effect is too small to observe, the matching effects on $T_m(H)$ and $J_c(H)$ are pronounced (see figures 2 and 3 below with the same label $l$).

Incidentally, this problem has much in common with the Frenkel–Kontorova and FVdM models [27], where competing periodicities of an elastic system and an underlying substrate can produce ground states of different periods. Domains can form when these uniform-ground-state mismatch energies between system and substrate exceed domain wall costs. The possibility of a rich structure in possible ground and metastable states can result due to the transition between commensurability and incommensurability in the vortex lattice and pin lattice, including devil's staircase parameter dependencies and dynamic effects of vortex-lattice relaxation against a

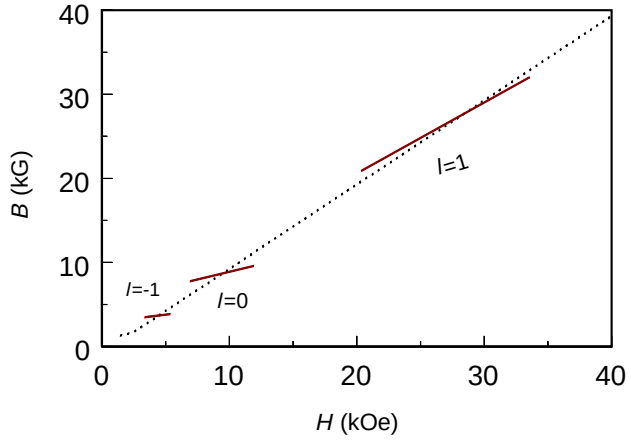


**Figure 1.** The constitutive $B$–$H$ relation is given for YBaCuO superconductors by equations (4) and (8) at fixed $T = 77$ K, with the parameters $\lambda(0) = 100$ nm, $\xi(0) = 1.4$ nm, $H_{c2}(0) = 170$ T, $T_c = 92$ K, $r_p = 7.5$ nm, $a_p = 50$ nm ($B_\Phi = 8.28$ kG). The solid lines represent the commensurate curves, showing the small-slope and lock-in transitions for $l = -1, 0, 1$. The dotted line represents the Abrikosov curve in the unpinned case (jumps are not shown).

periodic background [28]. It is much more reasonable to assume that energetically favourable structures may have domains with hexagonal lattices inside them and domain walls between them. Using the FVdM model [27] as a generic form to make an estimate, domains are disfavoured if the dimensionless domain density $\sim 1/L = \sqrt{V_p/\varepsilon_0}$ with relative domain size $L$ is not greater than the relative average mismatch of the two periodicity scales (of the vortex lattice and pin lattice) $\delta_{pq}/a_p$, where $\delta_{pq} = a_p - (p/q)a_0$ with integer $p$ and $q$. Thus the domain wall condition is $\delta_{pq} \leqslant a_p\sqrt{V_p/\varepsilon_0}$, showing a dependence on the depth of pinning. This simple estimate shows that domain-induced effects could occur if

$$1 - T/T_c \geqslant 2(\xi(0)/r_p)^2[\exp(r_p^2/a_p^2) - 1].$$

For high-$T_c$ materials with the parameters given above, domain formation occurs over a wide range of $1 - T/T_c > 10^{-3}$. Theoretically, all of the peculiarities of $B(H)$ curves including integer matching fields $B_{lm}/B_\Phi = \mu_{lm}^{\pm 2}$ and rational matching fields $B_{pq}/B_\Phi = p^2/q^2 = 9/4, 25/9, 25/4$ etc will arise if the potential $V_p$ is strong enough. For example, recent numerical simulations show [29] phase locking, Arnold tongues and devil's staircases in driven vortex lattices with periodic pinning. However, in an experiment only a few of the commensurate phases will be observable because of the finite resolution. This work focuses mainly on the integer matching fields and figures are produced for the matching fields $B_l/B_\Phi = 1/3, 1, 3$.

## 3. The elastic energy functional and the periodic pinning potential

Vortex lines have the reputation of leading to elastic forces which are modified by occasional spare pins [30]. On the other hand, thermal energy favours a vortex liquid of lines. Thus we need to consider an elastic energy functional and a periodic pinning potential. Vortex lines $i$, $j$ of transverse separation $\boldsymbol{r} = \boldsymbol{r}_i - \boldsymbol{r}_j$ interact via a screened potential in three-dimensional coordinate space given by $V(\boldsymbol{r}) = (1/r)\exp(-r/\lambda)$ with the coordinate of the vortex line segment $\boldsymbol{r}_i = (\boldsymbol{R}_i + \boldsymbol{u}_i(z), z)$ at $z$ displaced by an amount $\boldsymbol{u}_i(z)$ from its perfect hexagonal reference site $\boldsymbol{R}_i$. Here $\lambda$ is the London magnetic penetration depth in the $xy$-plane. Its Fourier

transform is given by $V(\boldsymbol{k}) = 1/[1 + \lambda^2(\boldsymbol{K}^2 + \varepsilon^2 k_z^2)]$ with $\boldsymbol{k} = (\boldsymbol{K}, k_z)$ and $\boldsymbol{K} = (k_x, k_y)$. Here $\varepsilon = \sqrt{m_{ab}/m_c} < 1$ is the ratio of the anisotropic Ginzburg–Landau masses. The momentum-space displacements are

$$u_\mu(\boldsymbol{k}) = a_0^2 \sum_i \int \mathrm{d}z \ \exp(-\mathrm{i}\boldsymbol{K}\cdot\boldsymbol{R}_i)\exp(-\mathrm{i}k_z z)u_i^\mu(z)$$

with $\mu = (x, y)$ where the integral is taken over all $z$ for a given vortex line $i$, and the sum is over all vortex lines. The inverse transform is

$$u_i^\mu(z) = \int_{-\infty}^{\infty} \frac{\mathrm{d}k_z}{2\pi} \int_0^{K_{BZ}^2} \frac{\mathrm{d}^2\boldsymbol{K}}{(2\pi)^2} \ \exp(\mathrm{i}\boldsymbol{K}\cdot\boldsymbol{R}_i)\exp(\mathrm{i}k_z z)u_\mu(\boldsymbol{k})$$

where the $\boldsymbol{K}$-integral is over the two-dimensional Brillouin zone, approximated by a circle of radius $K_{BZ} = \sqrt{4\pi}/a_0$ with unit-cell area $(\pi/4)a_0^2$. For the hexagonal lattice, the reference sites are $\boldsymbol{R}_i = (l\sqrt{3}a_0/2, (2l + m)a_0/2)$. Then an elastic energy functional can be obtained for small displacements in momentum space in terms of strain variables [11]:

$$E_{el}^{(1)} = \frac{1}{2}\int_{-\infty}^{\infty} \frac{\mathrm{d}k_z}{2\pi} \int_0^{K_{BZ}^2} \frac{\mathrm{d}^2\boldsymbol{K}}{(2\pi)^2} \ \left[c_{11}(\boldsymbol{k})|\boldsymbol{K}\cdot\boldsymbol{u}(\boldsymbol{k})|^2 + c_{66}|\boldsymbol{K}_\perp\cdot\boldsymbol{u}(\boldsymbol{k})|^2 + c_{44}(\boldsymbol{k})k_z^2|\boldsymbol{u}(\boldsymbol{k})|^2\right]. \tag{11}$$

Here $\boldsymbol{K}_\perp = (k_y, -k_x)$ and $c_{11}$, $c_{66}$ and $c_{44}$ are the compressional, shear and tilt elastic moduli of the vortex lattice in an isotropic medium. The simplest possible expressions for elastic moduli are

$$c_{11}(\boldsymbol{k}) \simeq \frac{c_{44}(\boldsymbol{k})}{\varepsilon^2} \simeq \frac{B^2/4\pi}{\varepsilon^2 + \lambda^2 K^2} \qquad c_{66} = \frac{B\phi_0}{(8\pi\lambda)^2}$$

due to the softening of the vortex lattice in high-$T_c$ superconductors. Quantum dissipation effects are also important below the intermediate $T$ and the elastic free energy including such effects in (11) is modified to [11] $E_{el} = E_{el}^{(1)} + E_{el}^{(2)}$, where

$$E_{el}^{(2)} = \frac{1}{2}\int_{-\infty}^{\infty} \frac{\mathrm{d}k_z}{2\pi} \int_0^{K_{BZ}^2} \frac{\mathrm{d}^2\boldsymbol{K}}{(2\pi)^2} \ \sum_n [\rho(\omega_n)\omega_n^2 + \eta(\omega_n)\omega_n]|\boldsymbol{u}_n(\boldsymbol{k})|^2 \tag{12}$$

and the displacement field $\boldsymbol{u}(z) \to \boldsymbol{u}(z, \tau)$ acquires an (imaginary) time dependence with the Matsubara frequency $\omega_n = 2\pi n k_B T/\hbar$. Here $\boldsymbol{u}_{n=0}(\boldsymbol{k})$ is the previous $\boldsymbol{u}(\boldsymbol{k})$ and $\rho(\omega_n)$ is the vortex mass per volume. The viscosity coefficient is $\eta(\omega_n) = \eta(0)/(1 + \omega_n\tau_r)$ where $\eta(0) = \phi_0 H_{c2}/\rho_N c^2 a_0^2$ is the vortex coefficient, $\rho_N$ is the normal-state resistivity and $\tau_r$ denotes an appropriate effective quantum relaxation time.

The pinning energy is taken to be parabolic in displacement from the minimum:

$$E_{pin} = \frac{1}{2}V_p\nu \sum_i \int_0^{L_z} \mathrm{d}z \ \left[\frac{1}{r_p^2}\left|\boldsymbol{\delta}_{pi} - \tilde{\boldsymbol{R}}_{pi}(z) + \boldsymbol{u}_i(z)\right|^2 - 1\right] \times \Theta(r_p - |\boldsymbol{\delta}_{pi} - \tilde{\boldsymbol{R}}_{pi}(z) + \boldsymbol{u}_i(z)|) \tag{13}$$

where $\tilde{\boldsymbol{R}}_{pi}(z)$ represents the transverse misalignment of columnar pins and possible 'straggling' of the columns along the $z$-axis. The elastic energy terms (11) and (12) are diagonalized in momentum space while the pinning energy term (13) is diagonal only in coordinate space. To carry out the functional integration in momentum space, one needs to approximate the Heaviside step function constraint to holding in an average sense (neglecting $\tilde{\boldsymbol{R}}_{pi}^2 \ll r_p^2$): $|\boldsymbol{u}_i + \boldsymbol{\delta}_{pi}|^2 < r_p^2$, through the following two steps. Firstly, since the equilibrium

variables $\boldsymbol{\delta}_{pi}$ (for $\boldsymbol{u}_i \simeq 0$) and the displacement variables $\boldsymbol{u}_i(z)$ (for any values of $\boldsymbol{\delta}_{pi}$) are independent each other, equation (13) can be simplified approximately to

$$E_{pin} = \frac{1}{2}\nu V_p\left(1 - \frac{\delta_p^2}{r_p^2}\right)\Theta(r_p - \delta_p)\sum_i \int_0^{L_z} \mathrm{d}z \left[\frac{1}{r_p^2}\left|\tilde{\boldsymbol{R}}_{pi}(z) - \boldsymbol{u}_i(z)\right|^2 - 1\right] \times \Theta(r_p - \boldsymbol{u}_i(z)). \tag{14}$$

Secondly, since the fluctuation $u_i$ has a Gaussian distribution, the probability is

$$\sim \exp\left[-\frac{1}{2}\beta(|\boldsymbol{u}_i|^2/r_p^2 - 1)\right]$$

if the constraint is satisfied and

$$\sim \exp\left[\frac{1}{2}\beta(|\boldsymbol{u}_i|^2/r_p^2 - 1)\right]$$

if it is not. So one can take the fraction with this Gaussian weight, normalized to these alternatives:

$$\Theta(r_p - u_i(z)) \simeq \frac{1}{1 + \exp\beta(\langle u_i^2\rangle/2r_p^2 - 1)} \equiv f(\langle u_i^2\rangle). \tag{15}$$

Substitution of $f$ for $\Theta(r_p - u_i(z))$ is a key approximation with $\beta$ a dimensionless constant of order unity. $f$, with a Fermi-like distribution, mimics the constraint of (14) and is some function interpolating between unity for $\langle u_i^2\rangle \ll 0$ and zero for $\langle u_i^2\rangle \gg 0$.

We assume that $\tilde{\boldsymbol{R}}_{pi}(z)$ is a random variable, $\langle \tilde{R}^{\mu}_{pi}(z)\rangle_{dis} = 0$ and its correlation function involves an $i$-dependent misalignment and a Gaussian distribution straggling along the $z$-direction:

$$\langle \tilde{R}^{\mu}_{pi}(z)\tilde{R}^{\mu'}_{pi'}(z')\rangle_{dis} = \bar{\sigma}_p^2 a_p^2 \delta_{ii'}\delta_{\mu\mu'}\exp[-(z - z')^2/2\bar{L}_p^2 r_p^2]. \tag{16}$$

Here $\bar{\sigma}_p, \bar{L}_p$ are dimensionless variables describing the disorder in the $xy$-plane and the correlation length in the $z$-direction, respectively. Since the elastic energy functionals (11) and (12) are Gaussian, one takes only a disorder average for $E_{pin}$ by use of the correlation function equation (16). One finally gets the total-energy functional in momentum space:

$$\begin{aligned} E_0 &= E_{el}^{(1)} + E_{el}^{(2)} + \frac{1}{2}\int_{-\infty}^{\infty}\frac{\mathrm{d}k_z}{2\pi}\int_0^{K_{BZ}^2}\frac{\mathrm{d}^2\boldsymbol{K}}{(2\pi)^2}\,\frac{\epsilon_p}{a_0^2}|\boldsymbol{u}(\boldsymbol{k})|^2 \\ \epsilon_p &\equiv \nu f\frac{V_p}{r_p^2}\left(1 - \frac{\bar{\sigma}_p^2}{\bar{\sigma}_{pc}^2}\right)\left(1 - \frac{\delta_p^2}{a_p^2}\right)\Theta(r_p - \delta_p) \\ \bar{\sigma}_{pc}^2 &\equiv \frac{k_B T r_p}{V_p a_p^2\sqrt{2\pi}\bar{L}_p}\exp[(k_z\bar{L}_p r_p)^2/2]. \end{aligned} \tag{17}$$

Although the pinning energy contribution is like a quantum contribution, it will affect both the thermal and quantum mean displacements. Equation (17) shows that the columnar disorder reduces the pinning strength, $V_p \to V_p(1 - \bar{\sigma}_p^2/\bar{\sigma}_{pc}^2)$, and acts like a zero pin for $\bar{\sigma}_p$ greater than its critical value $\bar{\sigma}_{pc}$.

## 4. Inhibition of vortex-lattice melting with hexagonal columnar pins and its encouragement with an applied current drive

The melting temperature depends dramatically both on the flexibility of the lines and the ratio of pinning energy to elastic energy. The mean square displacement amplitude

$$\langle|\boldsymbol{u}_i|^2\rangle = \sum_{n,k}\langle|\boldsymbol{u}_n(\boldsymbol{k})|^2\rangle \equiv d_p^2$$

can be expressed as

$$d_p^2 = \left(\int \mathcal{D}[u]\ \sum_n |\boldsymbol{u}_n|^2 \exp(-E_0/k_BT)\right)\Big/\left(\int \mathcal{D}[u]\ \exp(-E_0/k_BT)\right)$$
$$= k_BT \sum_n \int_{-\infty}^{\infty} \frac{\mathrm{d}k_z}{2\pi} \int_0^{K_{BZ}^2} \frac{\mathrm{d}^2\boldsymbol{K}}{(2\pi)^2} \left(\frac{1}{c_{11}(\boldsymbol{k})\boldsymbol{K}^2 + c_{44}(\boldsymbol{k})k_z^2 + \eta(\omega_n)|\omega_n| + \epsilon_p/a_0^2}\right.$$
$$\left. + \frac{1}{c_{66}\boldsymbol{K}^2 + c_{44}(\boldsymbol{k})k_z^2 + \eta(\omega_n)|\omega_n| + \epsilon_p/a_0^2}\right) \tag{18}$$

from transverse and longitudinal components. Following Blatter *et al* [8,11], I use the simplest formula to deduce the mean square displacement amplitude. First, consider the thermal term ($n = 0$); the result is

$$(d_p^{(T)})^2 = (d_0^{(T)})^2 p_{red}. \tag{19}$$

Here

$$(d_0^{(T)})^2 = \sqrt{\frac{G_i}{\beta_m}} \frac{\sqrt{b}t}{1-t-b} a_0^2$$

is the zero-pin mean square displacement amplitude [8, 11] with the Ginzburg number

$$G_i = \frac{1}{8}[k_BT_c/\varepsilon\varepsilon_0(0)\xi(0)]^2$$

and numerical factor $\beta_m \simeq 5.6$. Where I have simplified the integral formula, the detailed calculations merely change the value of $\beta_m$ [6, 8]. With $k_z = \pi/\bar{L}_p r_p$, the reduction factor is

$$p_{red} \equiv \sqrt{1+p} - p\ln[(1+\sqrt{1+p})/\sqrt{p}] \tag{20}$$

where

$$p \equiv \frac{\epsilon_p}{4\pi c_{66}} = \frac{\sqrt{3}\nu f a_0^2}{2\pi r_p^2}\left(1 - \frac{\bar{\sigma}_p^2}{\bar{\sigma}_{pc}^2}\right)\left(1 - \frac{\delta_p^2}{a_p^2}\right)\Theta(r_p - \delta_p)\ln\left(1 + \frac{r_p^2}{2\xi^2(t)}\right)$$

represents the ratio of pinning energy to elastic energy. This is a key parameter and varies from zero (zero pins) to $\gg 1$ (strong pins). For commensurate regimes, the thermal fluctuation magnitudes are reduced by the factor $p_{red}$, and $p_{red} \simeq 1 - p\ln 2$ for $p \ll 1$ and $p_{red} \simeq 2/3\sqrt{p}$ for $p \gg 1$.

The quantum contribution ($n \neq 0$) is dominated by single-vortex fluctuations at $K \sim K_{BZ}$; the result is

$$(d_p^{(Q)})^2 = \frac{(d_0^{(Q)})^2}{1 + T_Q/T}. \tag{21}$$

Here $(d_0^{(Q)})^2 \simeq 4\nu_0\xi/\pi^2 K_F$ is the zero-pin mean square displacement amplitude [8, 11] with the Fermi wave vector $K_F \simeq 1.5$–$2.0\ \mathrm{nm}^{-1}$ and numerical factor $\nu_0 \simeq 4$ [8]. The quantum characteristic temperature $T_Q$ is

$$T_Q = \frac{\phi_0^2 e^2 \rho_N \nu f}{16\pi^4 r_p^2 \hbar k_B \kappa^2}\left(1 - \frac{\bar{\sigma}_p^2}{\bar{\sigma}_{pc}^2}\right)\left(1 - \frac{\delta_p^2}{a_p^2}\right)\Theta(r_p - \delta_p)\ln\left(1 + \frac{r_p^2}{2\xi^2}\right)$$

below which quantum tunnelling is suppressed by the hexagonal lattice of columnar pins. Since $T_Q \ll T_m$ [13], we can ignore this effect.

Combining thermal and quantum contributions, I obtain

$$d_p^2 = (d_p^{(T)})^2 + (d_p^{(Q)})^2 = \sqrt{\frac{G_i}{\beta_m}} \frac{\sqrt{b}t}{1-t-b} a_0^2 p_{red} + \frac{4\nu_0\xi(0)}{\pi^2 K_F \sqrt{1-t-b}}. \tag{22}$$

Extending the Lindemann melting criterion, the vortex lattice becomes unstable and melts when $d_p$ reaches an appreciable fraction $c_L \simeq 0.1$–$0.3$ of the scale lattice constant $a_0$ ($a_p$) for $B \geqslant B_\Phi$ ($B < B_\Phi$):

$$d_p^2 = \nu c_L^2 a_p^2. \tag{23}$$

It is actually more convenient to determine the melting line as $B_m(T)$ by solving the equation

$$t = 1 - b_m - \frac{\xi^2(0)}{\nu c_L^2 a_p^2}\left[2\pi t p_{red}\sqrt{\frac{G_i}{\beta_m b_m}} + \frac{4\nu_0}{\pi^2 \xi(0) K_F}\sqrt{1 - t - b_m}\right]. \tag{24}$$

In general, $f$ depends on $d_p^2$ and is thus evaluated self-consistently. For the vortex-lattice melting, however, one can use $f = f(\nu c_L^2 a_p^2)$ in this case. Alternately, from equation (24) one can get its inverse form $T_m(B)$ and further obtain the melting line $T_m[B(H)]$ by use of equations (4) and (8). Clearly, since $p_{red} < 1$ for commensurate regimes, the melting line is pushed to higher temperatures.

With the following choice of parameters for the YBaCuO system: $\lambda(0) = 100$ nm, $\xi(0) = 1.4$ nm, $\varepsilon = \frac{1}{5}$, $T_c = 92$ K, $H_{c2}(0) = 170$ T (so $G_i = 4 \times 10^{-3}$), $K_F \simeq 1.7$ nm$^{-1}$ [8], $\beta_m = 5.6$, $\nu_0 = 4$, $\beta = 1$, $r_p = 7.5$ nm and $a_p = 50$ nm ($B_\Phi = 8.28$ kG), and the fitting parameter $c_L = 0.2$ for the zero-pin case [8, 31] and $\bar{\sigma}_p = 0$ (without disorder), figure 2 shows the melting line $T_m(H)$ (solid line). This line rises sharply on going from $B$ outside the commensurate region to $B$ inside the small-slope region for $l = -1, 0, 1$. Roughly, $T_m \simeq T_c/(1 + 0.05 p_{red})$ at $B = B_\Phi$, well below $T_c$. The increase of 10% in $T_m$ agrees with the observation [19] excellently, in which $B_m(T)$ shows a series of cusps with $\mu_{l0}^2 = l$ ($l = 1, 2, 3, \ldots$).

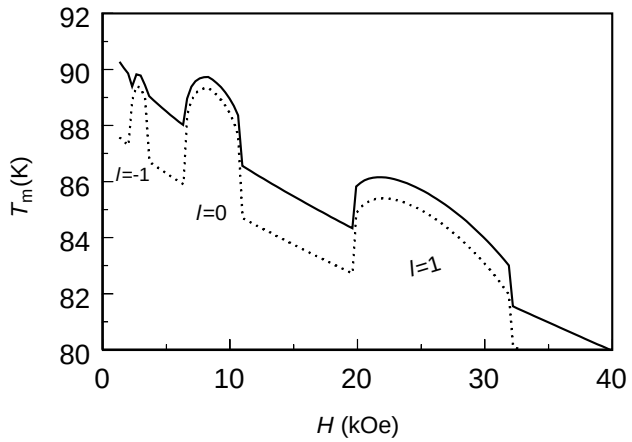


**Figure 2.** The curve of the melting temperature $T_m$ versus the external field $H$ is given by equations (24), (4) and (10), with the parameters $\varepsilon = \frac{1}{5}$, $\beta_m = 5.6$, $\nu_0 = 4$, $K_F = 1.7$ nm$^{-1}$, $c_L = 0.20$, $\beta = 1$ and $\bar{\sigma}_p = 0$. The solid line represents the curve in the absence of a current drive ($J = 0$). The dotted line represents the equation (24) curve modified by equation (28) for $J = 1 \times 10^5$ A cm$^{-2}$. In the pinned case, there are three plateaus for $B = -1, 0, 1$ (the curve with disorder is not shown). In the unpinned case, as a special example, the shape of the melting line is well described by the single remaining parameter $c_L = 0.20$.

Now consider $x$-directional current-$J$ drive effects. $J$ is like a topological 'electric field' with a linear potential energy additional to equation (17):

$$E = E_0 - \sum_i \int_0^{L_z} \frac{\phi_0}{c} J u_i^y \, \mathrm{d}z. \tag{25}$$

Since $E_0[u]$ is Gaussian, one can easy obtain the statistical partition function:

$$Z = \int \mathcal{D}[u]\ \exp(-E/k_BT) = Z_0 \exp\left[\langle u_y^2\rangle_0 \frac{1}{2}\left(\frac{\phi_0 J L_z}{ck_BT}\right)^2\right] \tag{26}$$

with subscript zero denoting the absence of $J$. From $\langle u_y\rangle \propto \partial Z/Z\,\partial J$ and $\langle u_y^2\rangle \propto \partial^2 Z/Z\,\partial J^2$, I get

$$\langle u_y\rangle = \frac{\phi_0 J L_z}{ck_BT}\langle u_y^2\rangle_0 \qquad \langle u_y^2\rangle = \langle u_y^2\rangle_0 + 2\langle u_y^2\rangle_0^2\left(\frac{\phi_0 J L_z}{ck_BT}\right)^2.$$

Since $\langle u_x^2\rangle_0 = \langle u_y^2\rangle_0 = \frac{1}{2}\langle u^2\rangle_0 = \frac{1}{2}d_p^2$, I have

$$\langle u^2\rangle = \langle u_x^2\rangle_0 + \langle (u_y - \langle u_y\rangle)^2\rangle = d_p^2\left[1 + d_p^2\left(\frac{\phi_0 J L_z}{2ck_BT}\right)^2\right]. \tag{27}$$

Using the criterion of melting with $J \neq 0$, equation (24) is modified to

$$t = 1 - b_m - \frac{\xi^2(0)}{\nu c_L^2 a_p^2}\left[1 + d_p^2\left(\frac{\phi_0 J L_z}{2ck_BT}\right)^2\right]\left[2\pi t p_{red}\sqrt{\frac{G_i}{\beta_m b_m}} + \frac{4\nu_0}{\pi^2\xi(0)K_F}\sqrt{1 - t - b_m}\right]. \tag{28}$$

Figure 2 also shows the melting line $T_m(H, J)$ (dotted line), from equation (28), for $J = 1 \times 10^5$ A cm$^{-2}$ with $L_z = 2a_p = 100$ nm. This line shifts downwards and the shifting is smaller within the pinned region than outside the pinned region. Current encourages melting while pinning inhibits melting. In the special case of the absence of columnar pins, on setting $p = 0, \nu = B_\Phi/B$ and $H = H_A(B)$ in the above formulae, the plateaus disappear in the curves of $T_{m0}(H, J)$, like in the early works [8, 31].

## 5. Enhancement of critical current density with hexagonal columnar pins and its destruction with columnar pin disorder

This section will address a possible mechanism for the commensurate enhancement of the critical current density $J_c$ due to the periodic columnar defects. The matching effect is easily observed by examining the experimental $J_c(H)$ curve. The mean columnar pin force, up to numerical constants, is given by $V_p r_p/2L_z d_p$ acting on trapped vortices, with $r_p/d_p$ the fluctuation effect [11]. $J_c$ is simply determined by equating the pinning forces with the Lorentz forces $J_c\phi_0 a_p^2/ca_0^2$ acting on all vortices in the area $a_0^2$:

$$J_c \simeq cV_p r_p a_0^2/2\phi_0 L_z a_p^2 d_p. \tag{29}$$

Substituting $d_p$ of equation (22) into equation (29), the explicit formula for $J_c$ is

$$J_c(T, B) = \frac{\pi c\varepsilon_0(0)\xi(0)r_p}{2\phi_0 a_p^3}\ln[1 + r_p^2/2\xi^2(t)] \times (1 - t - b)^{3/2}\Big/\left[2\pi b t p_{red}\sqrt{\frac{G_i b}{\beta_m}} + \frac{4\nu_0 b^2}{\pi^2\xi(0)K_F}\sqrt{1 - t - b}\right]^{1/2} \tag{30}$$

which is still self-consistent with $f$. However, since $f \sim 1$, this calculation is easy to do numerically.

Combining equation (30) with equations (4) and (8) and using the same parameters as above, in figure 3 I show $J_c$ versus $H$ at fixed $T = 77$ K without disorder (solid line) and with disorder $\bar{\sigma}_p = 0.16$ (dotted line) for $\bar{L}_p = 1$. It is reasonable to expect the difference in

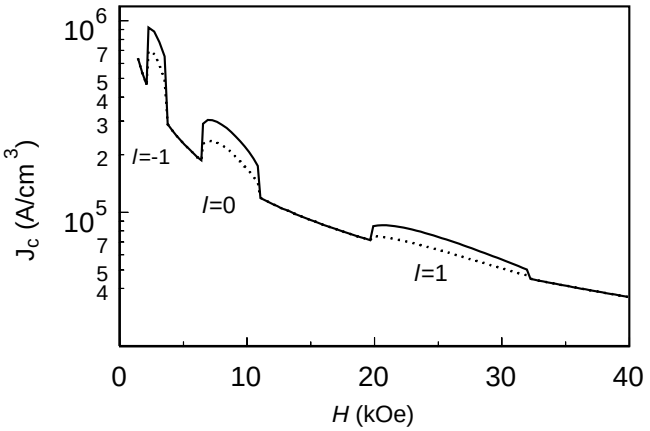


**Figure 3.** The curve of the critical current density $J_c$ versus the external field $H$ is given for YBaCuO superconductors by equations (30), (4) and (8) at fixed $T = 77$ K. The parameters chosen are $\lambda(0) = 100$ nm, $\xi(0) = 1.4$ nm, $H_{c2}(0) = 170$ T, $T_c = 92$ K, $\varepsilon = \frac{1}{5}$, $\beta_m = 5.6$, $\nu_0 = 4$, $K_F = 1.7$ nm$^{-1}$, $r_p = 7.5$ nm, $a_p = 50$ nm ($B_\Phi = 8.28$ kG) and $\beta = 1$. The solid line represents the curve in the absence of disorder ($\bar{\sigma}_p = 0$). The dotted line represents the curve with non-zero disorder $\bar{\sigma}_p = 0.16$. For commensurate regimes, there are three plateaus for $l = -1, 0, 1$. For incommensurate regimes ($p = 0$), this small $J_c$ corresponds to weak pins.

$J_c$ between the cases with and without columnar defects due to columnar pinning. Note that $J_c(H)$ shows a series of plateaus when the magnetic flux lattice is commensurable with the columnar pin lattice and figure 3 only shows those for $l = -1, 0, 1$. Roughly, $J_c(p \neq 0)/J_c(p = 0) \simeq 1/\sqrt{p_{red}}$ and this ratio is about 2.0 at $B = B_\Phi$. Compared to random pinning [1, 11], regular pinning leads to a marked enhancement of $J_c$. This is similar to the finding from the calculation of the magnetization [32]. The dotted line shows that the introduction of disorder shifts $J_c$ towards lower values and washes out the plateau when the disorder reaches a characteristic value. The relative suppression of the plateaus is stronger for $l = 1$ than for $l = 0$ and $-1$. This is because the plateau for $l = 1$ near $B = 3B_\Phi$ is caused by more weakly pinned interstitial vortices, which are more susceptible to disorder. This $J_c(H)$ curve is one of my key results.

It is interesting to calculate $J_c(T)$ at $B = B_\Phi$, the balance between regular pinning and thermal fluctuation. The solid line in figure 4 shows this behaviour, displaying $J_c \sim (1 - T/T_c)^{3/2}$ at intermediate temperatures as expressed explicitly in equation (30) and $J_c$ exponentially vanishing at high temperatures with increasing temperature. This behaviour agrees well with analysis [11] and observation [19]. The $(1-T/T_c)^{3/2}$ dependence of $J_c$ is also the signature of columnar defect pinning [21]. Thermal fluctuations have smoothed the weak pinning potential at high temperatures, so $J_c$ decreases rapidly with increasing temperature, while the regular pinning retains more efficiency with thermal fluctuations at intermediate temperatures, resulting in a power-3/2 decay of $J_c$ with increasing temperature. The dotted line in figure 4 shows the $J_c(T)$ curve with disorder $\bar{\sigma}_p = 0.16$ at $B = B_\Phi$, indicating a marked decrease in $J_c$ below intermediate temperatures due to disorder effects.

## 6. Summary

The presence of a regular lattice of columnar defects is not only technologically relevant but also provides the framework for the physical realization of novel thermodynamical phases

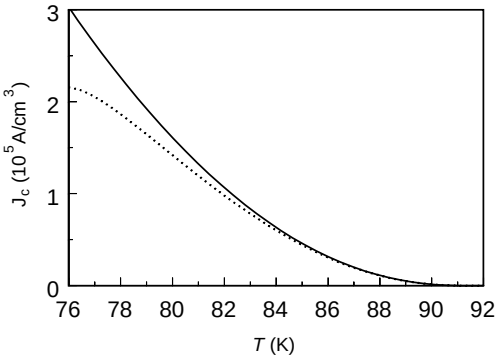


**Figure 4.** The $J_c$–$T$ curve at $B = B_\Phi$ (the other parameters are the same as in figure 3).

such as commensurability and multiple Bose glasses. The strong periodic pinning introduces additional new features into the thermodynamic phase diagram—such as the creation of new small-slope transitions, the inhibition of vortex-lattice melting and the enhancement of critical current density, as well as the appearance of their plateaus. In this work, I have investigated the effects of a hexagonal lattice of columnar defects on the curves of the magnetic induction $B(H)$, vortex-lattice melting $T_m(H)$ and critical current density $J_c(H)$. The vortex–vortex interaction, thermal and quantum fluctuations, an applied current drive and columnar pin disorder have been taken into account. By use of the Gibbs free-energy minimum, through the exact analysis of the vortex interaction, the $B(H)$ curve has been calculated. Under the elastic approximation, the $T_m(H)$ curve has been estimated using the extended Lindemann criterion. By means of a dimensional estimation, the $J_c(H, T)$ curves have been plotted. The results clearly show that the balance between the vortex-pin commensurability and thermal/quantum fluctuations produces in $J_c$ a marked increase, shifts the experimentally observed $T_m$ towards higher values and also leads to a series of plateaus in $J_c(H)$ and $T_m(H)$ curves. The applied current drive encourages vortex-lattice melting. This occurs mainly in the regions of incommensurate field and it is hard to destroy the plateaus within the commensurate regions. The balance between the best matching at $B = B_\Phi$ and thermal fluctuations produces in $J_c$ a power-$3/2$ decay with temperature at intermediate temperatures and an exponential vanishing close to $T_c$. The delta-correlated columnar pin disorder with a Gaussian distribution destroys all of these favourable effects and washes out all plateaus when it is greater than its critical value. It needs pointing out, finally, that this approach is not only suitable for high-$T_c$ superconductors but also works especially well for conventional superconductors at the spatial scale accessible to experimental investigations.

## Acknowledgments

This work was performed as projects 19834010 and 19575009, supported by National Natural Science Foundation of China. I am grateful to Professor Subodh R Shenoy for providing many suggestions and detailed calculations during my visit to ICTP, Italy.

## References

[1] Civale L *et al* 1991 *Phys. Rev. Lett.* **67** 648
Konczykowski M *et al* 1991 *Phys. Rev.* B **44** 7167
Krusin-Elbaum L *et al* 1996 *Phys. Rev. Lett.* **76** 2563
[2] Budhani R C, Suenaga M and Liou S H 1992 *Phys. Rev. Lett.* **69** 3816

[3] Nelson D R and Vinokur V 1992 *Phys. Rev. Lett.* **68** 2398
Nelson D R and Vinokur V 1993 *Phys. Rev.* B **48** 13 060
[4] Nelson D R 1988 *Phys. Rev. Lett.* **60** 1973
Brandt E H 1989 *Phys. Rev. Lett.* **63** 1106
[5] Safar H *et al* 1992 *Phys. Rev. Lett.* **69** 824
Welp U *et al* 1996 *Phys. Rev. Lett.* **76** 4809
[6] Houghton A, Pelcovits R A and Sudbo A 1989 *Phys. Rev.* B **40** 6763
[7] Brandt E H *et al* 1993 *Phys. Rev.* B **48** 15 914
[8] Blatter G and Ivlev B 1993 *Phys. Rev. Lett.* **70** 2621
Blatter G and Ivlev B 1994 *Phys. Rev.* B **50** 10 272
[9] Jensen H and Brass A 1990 *Phys. Rev.* B **41** 6394
Koshelev A and Vinokur V 1994 *Phys. Rev. Lett.* **73** 3580
[10] Kwok W K, Fendrich J A, van der Beek C J and Crabtree G W 1994 *Phys. Rev. Lett.* **73** 2614
[11] Blatter G *et al* 1994 *Rev. Mod. Phys.* **66** 1125
[12] Crabtree G W and Nelson N R 1997 *Phys. Today* **50** (4) 38
[13] Ma Y L and Shenoy S R 2000 *Physica* C submitted
[14] Reichhardt C *et al* 1996 *Phys. Rev.* B **54** 16 108
Reichhardt C, Olson C J and Nori F 1997 *Phys. Rev. Lett.* **78** 2648
Reichhardt C, Olson C J and Nori F 1998 *Phys. Rev.* B **58** 6534
Gurevich A, Kadyrov E and Larbalestier D C 1996 *Phys. Rev. Lett.* **77** 4078
[15] Brandt E H 1995 *Rep. Prog. Phys.* **58** 1465
[16] Fiory A T, Hebard A F and Somekh S 1978 *Appl. Phys. Lett.* **32** 73
[17] Metlushko V V 1994 *Solid State Commun.* **91** 331
[18] Baert M *et al* 1995 *Phys. Rev. Lett.* **74** 3269
[19] Lykov A N 1993 *Solid State Commun.* **86** 531
[20] Cooly L D *et al* 1994 *Appl. Phys. Lett.* **64** 1298
[21] Lin J-Y *et al* 1996 *Phys. Rev.* B **54** R12 717
[22] Buzdin A I 1993 *Phys. Rev.* B **47** 11 416
[23] Fetter A L and Hohenburg P C 1969 *Superconductivity* vol 2, ed R D Parks (New York: Dekker) p 836
[24] Fetter A L, Hohenburg P C and Pincus P 1966 *Phys. Rev.* **147** 140
Fetter A L 1966 *Phys. Rev.* **147** 153
[25] Feinberg D and Villard C 1990 *Phys. Rev. Lett.* **65** 919
Bulaevskii L N and Clem J R 1991 *Phys. Rev.* B **44** 10 234
[26] Brandt E H and Essmann U 1987 *Phys. Status Solidi* b **144** 13
[27] Bak P 1982 *Rep. Prog. Phys.* **45** 587
[28] Martinoli P 1978 *Phys. Rev.* B **17** 1175
[29] Reichhardt C and Nori F 1999 *Phys. Rev. Lett.* **82** 414
[30] Khalfin I B and Shapiro B Ya 1993 *Physica* C **207** 359
[31] de Andrade R Jr and de Lima O F 1995 *Phys. Rev.* B **51** 9383
[32] Dasgupta C and Feinberg D 1998 *Phys. Rev.* B **57** 11 730